

# Sensor Validation for Structural Systems with Additive Sensor Faults

Maher Abdelghani<sup>1,\*</sup> and Michael I. Friswell<sup>2</sup>

<sup>1</sup>*Department of Engineering Physics, INSAT, Centre Urbain, Tunis Nord, BP 676, 1080 Tunis cedex, Tunisia*

<sup>2</sup>*Department of Aerospace Engineering, University of Bristol, Queen's Building, University Walk, Bristol BS8 1TR, UK*

Structures with a large number of sensors and actuators are becoming more common, and their applications vary from active control to damage location. This large amount of spatial information should be used to advantage to continuously monitor the correct functioning of the sensors during normal operation. Errors introduced by faulty sensors can cause a loss of performance and erroneous conclusions, and this paper analyses additive sensor faults. Two residual generation schemes are proposed to monitor sensor faults, namely the modal filtering approach and the so-called Parity Space approach. These residuals are then tested using a probabilistic approach using a  $\chi^2$  test to determine if there is a faulty sensor. These approaches are demonstrated on a simulated cantilevered beam excited at its tip and also on an experimental subframe structure.

**Keywords** sensor validation · parity space · modal space · residuals

## 1 Introduction

Smart structures have the potential to place a large number of distributed actuators and sensors on a structure. The correct functioning of active control and health monitoring requires that the sensors are functioning. Errors introduced by faulty sensors can cause undamaged areas to be identified as damaged, or control system performance to be inadequate, or certainly less than optimal. In many civil structures applications of health monitoring (such as bridges), ambient loads must be used for excitation. These loads are not known and may be measured or estimated as part of the health monitoring algorithm, which requires a large number of sensors.

Sensor validation, where the sensors are confirmed to be functioning during operation, seems to have received little attention in the smart structures and structural health monitoring communities. The critical aspect in smart structures is that there are usually more sensors than excited modes. This redundancy may be used, together with a model of the structure, to validate the sensor functionality.

The control and chemical engineering community have considered the sensor validation problem, and have used models and sensor redundancy to good effect. However, these approaches usually use the faulty sensor to predict the response and look for errors between predictions and measurement, although using the faulty

\*Author to whom correspondence should be addressed.  
E-mail: Maher.Abdelghani@insat.rnu.tn

sensor in the prediction process will propagate errors to the predicted responses. Often neural networks, or artificial intelligence approaches are used for the analysis.

Friswell and Inman [7] assumed that only the lower modes of the structure are usually excited, producing a large redundancy in the data. This has similarities to the principal component analysis used in chemical plant [5,6,14]. The alternative, used here, is to generate the residuals using the parity space approach [3,4] or by using modal residuals [7]. The approach is demonstrated on a beam structure, although the method is completely general and may be applied to any structure for which a model is available. If necessary, such a model could be obtained from an identification experiment.

Faults may cause a variety of changes in the dynamic response of a sensor, and many of these are difficult to model. However the two most common faults, namely additive and multiplicative faults, are relatively straightforward to model. Physically additive faults might arise from DC offsets in the electronic equipment and multiplicative faults might arise from calibration errors. In this paper the sensor faults are assumed to be additive and modeled as a constant signal added to the sensor response. The problem of detecting sensor faults is then transformed into the problem of the detection of the change in the mean of a Gaussian variable with known covariance matrix, which switches from zero under the no-fault condition to a mean value with unknown magnitude under the fault condition. This problem may be solved using a likelihood ratio test resulting in a  $\chi^2$  distributed variable, which is then compared to a threshold. In order to decide which sensor or subset of sensors is most likely to be responsible for the fault, the so-called sensitivity tests are computed, which are also  $\chi^2$  distributed.

## 2 Sensor Validation Concepts

Although there is redundancy in the data, based on the number of sensors and the number of modes excited, it is still not straightforward to identify those sensors that are damaged. When all

sensors are working, it is possible to estimate the modal contributions to the response and therefore produce a predicted response that will give some idea of the accuracy of the model of the structure and the extent of the measurement noise. However if a sensor is damaged, then using data from this sensor to estimate the modal participation factors will propagate the errors from the faulty channel through the estimate of the modal response to the estimate of the response in all channels. Thus to predict faulty sensors the sensors are split into two groups. If  $S$  represents the set of all sensors then the two groups are,

$$\begin{aligned} S_f &= \{\text{sensors assumed to be faulty}\} \\ S_w &= \{\text{sensors assumed to be working}\} \end{aligned}$$

Note that these two sets are disjoint so that

$$S_f \cap S_w = \{\} \quad S_f \cup S_w = S.$$

Note that the distribution of faulty and working sensors seems to have been determined at the outset. In practice, the sensors that are faulty will be unknown and so every potential subset of faulty sensors must be tried. This approach has parallels with the subset selection technique in parameter estimation [8,9,12]. The difficulty in sensor validation, as in parameter estimation, is to determine which sensor or parameter subset is optimal. Note that for sensor validation, the number of assumed working sensors should be at least as great as the number of modes of interest.

## 3 The Dynamic Model

The theory is best developed using the discrete time equations of motion in state space form. The development follows Basseville [3] closely. The equations of motion for the functioning system are, for some constant matrices  $A$ ,  $B$ ,  $C$ , and  $D$ , of appropriate dimension,

$$\begin{aligned} X_{k+1} &= AX_k + BU_k + W_k \\ Y_k &= CX_k + DU_k + V_k \end{aligned} \quad (1)$$

where  $X_k \in \mathbb{R}^{2n}$ ,  $Y_k \in \mathbb{R}^r$ , and  $U_k \in \mathbb{R}^m$  are the state vector, the output, and the controlled input at discrete time  $k$ .  $n$  is the number of degrees of freedom of the system,  $r$  is the number of outputs, and  $m$  is the number of force inputs.  $W_k$  and  $V_k$  denote two random noise sequences.

Most structural models are defined in continuous time and defined using mass, damping, and stiffness matrices, although the model may be transformed to discrete time. The measured data is sampled, and this motivates the use of discrete time equations. The second-order equations of motion are given by

$$\hat{M}\ddot{q} + \hat{C}\dot{q} + \hat{K}q = f = \hat{F}u \quad (2)$$

where  $q(t) \in \mathbb{R}^n$  is the vector of generalized co-ordinates,  $f(t) \in \mathbb{R}^n$  is the external force in physical coordinates,  $u(t) \in \mathbb{R}^m$  is the system input, and  $\hat{F} \in \mathbb{R}^{n \times m}$  determines the location of the applied force input.  $\hat{M}, \hat{C}, \hat{K} \in \mathbb{R}^{n \times n}$  are the mass, damping, and stiffness matrices, respectively. This may be written in continuous state space form as

$$\begin{aligned} \dot{x} &= \begin{bmatrix} 0 & I \\ -\hat{M}^{-1}\hat{K} & -\hat{M}^{-1}\hat{C} \end{bmatrix} x + \begin{bmatrix} 0 \\ \hat{M}^{-1}\hat{F} \end{bmatrix} u \\ &= \hat{A}x + \hat{B}u \end{aligned} \quad (3)$$

where the state vector is

$$x = \begin{Bmatrix} q \\ \dot{q} \end{Bmatrix}, \quad (4)$$

and  $\hat{A}$  and  $\hat{B}$  are defined in Equation (3). Integrating Equation (3) from time  $t_k$  to  $t_{k+1}$ , assuming that the input is constant and given by  $U_k$ , gives Equation (1) where [11],

$$A = \exp \hat{A} \delta t, \quad B = \left[ \int_0^{\delta t} \exp \hat{A} \tau d\tau \right] \hat{B} \quad (5)$$

and  $\delta t = t_{k+1} - t_k$ . In the output equation, the second of Equation (1),  $C$  determines which displacements are measured.  $D$  is usually zero, although  $D$  will be nonzero if acceleration is measured.

Suppose that the system is faulty, so that the faulty system is assumed to have the following equations of motion,

$$\begin{aligned} X_{k+1} &= AX_k + BU_k + \Gamma F_X + W_k \\ Y_k &= CX_k + DU_k + \Xi F_Y + V_k \end{aligned} \quad (6)$$

where  $F_X \in \mathbb{R}^{q_X}$  and  $F_Y \in \mathbb{R}^{q_Y}$  are the assumed additive faults. These faults are assumed constant, but unknown. The matrices  $\Gamma$  and  $\Xi$  are assumed known and determine the location of possible faults.

Assume that  $Y$  and  $U$  are measured over a finite time window of size  $p$ . Let

$$Y_k^{(p)} = \begin{Bmatrix} Y_{k-p+1} \\ Y_{k-p+2} \\ \vdots \\ Y_k \end{Bmatrix}, \quad U_k^{(p)} = \begin{Bmatrix} U_{k-p+1} \\ U_{k-p+2} \\ \vdots \\ U_k \end{Bmatrix}, \quad (7)$$

then, from Equation (6), by repeatedly substituting the first of Equation (6) into the second,

$$\begin{aligned} Y_k^{(p)} &= O_p X_{k-p+1} + M_p(B, D) U_k^{(p)} + M_X(\Gamma) F_X \\ &\quad + M_Y(\Xi) F_Y + Z_k^{(p)} \end{aligned} \quad (8)$$

where the observability matrix is

$$O_k^{(p)} = \begin{bmatrix} C \\ CA \\ \vdots \\ CA^{p-1} \end{bmatrix} \quad (9)$$

and

$$\begin{aligned} &M_p(B, D) \\ &= \begin{bmatrix} D & 0 & 0 & \cdots & 0 & 0 \\ CB & D & 0 & \cdots & 0 & 0 \\ CAB & CB & D & \cdots & 0 & 0 \\ \vdots & \vdots & \vdots & \ddots & \vdots & \vdots \\ CA^{p-2}B & CA^{p-3}B & CA^{p-4}B & \cdots & CB & D \end{bmatrix}. \end{aligned} \quad (10)$$

The coefficients of the faults are

$$M_X(\Gamma) = \begin{bmatrix} 0 \\ C \\ CA + C \\ \vdots \\ CA^{p-2} + \dots + CA + C \end{bmatrix} \Gamma \quad (11)$$

and

$$M_Y(\Xi) = \begin{bmatrix} \Xi \\ \Xi \\ \vdots \\ \Xi \end{bmatrix}. \quad (12)$$

The noise sequences have combined to give

$$Z_k^{(p)} = M_p(I_n, 0) W_k^{(p)} + V_k^{(p)}. \quad (13)$$

The purpose of Equation (8) is to collate all the information for the time window into a single equation. It is instructive to summarize the known and unknown quantities in Equation (8). Assuming that the model of the structure is known, then  $O_k^{(p)}$ ,  $M_p$ ,  $M_X$ , and  $M_Y$  will be determined. The unknown quantities are  $X_{k-p+1}$ , which are the initial conditions for the time window, the quantities relating to the fault,  $F_X$  and  $F_Y$ , and the random noise  $Z_k^{(p)}$ .

#### 4 The Parity Space Approach to Residual Generation

Given the measured quantities, one could minimize the unknown random noise,  $Z_k^{(p)}$ , in Equation (8), and identify  $F_X$  and  $F_Y$ , together with  $X_{k-p+1}$ , and the performance of this estimation would depend on the statistical properties of the noise. The parity space method takes a different approach. The observability matrix,  $O_p$ , has dimension  $(2pn \times r)$ . Since  $r \leq 2n$ , this matrix has a large null space. Let  $N$  be any matrix such that

$$N^T O_p = 0 \quad (14)$$

and if the system is observable then the maximum size of  $N$  is  $2pn \times (2pn - r)$ . The columns of  $N$  define the parity space. The vector parity check then produces residuals as

$$\varepsilon_k = N^T [Y_k^{(p)} - M_p(B, D)U_k^{(p)}], \quad (15)$$

since if there are no faults then this expression just gives a combination of the random noise (compare to Equation (8)). A fault is detected if this expression is not zero.

The parity check given by Equation (15) uses all the columns of  $N$ . It is also possible to use a subspace of the null space. Furthermore  $N$  is not unique, since there are many matrices whose columns will span a given null space. Making the columns of  $N$  an orthonormal basis of the parity space is likely to be a good idea, and the singular value decomposition of the observability matrix is a convenient method to calculate such a basis. In the following example a full rank parity check is performed, that is the dimension of the parity space is as large as possible.

The development thus far has assumed that the input force is known. An alternative, if the locations of the external forces can be determined, is to ensure that

$$N^T M_p(B, D) = 0 \quad (16)$$

in addition to Equation (14). However, this is only sensible if the rank (and hence the number of columns) in  $B$  is relatively small. In the example the impulse response is used, where the external force is zero after the initial impact.

#### 5 The Modal Filtering Approach

The approach suggested by Friswell and Inman [7] was based on the assumption that the response was contained in the subspace spanned by the lower modes of the structure. Although, in general, the modes will be complex for non-proportional damping, for lightly damped structures the undamped modes provide a good

approximation for the response subspace [10]. Thus, the response may be written as

$$q(t) = \sum_{i=1}^n \phi_i p_i(t) \quad (17)$$

where  $\phi_i \in \mathbb{R}^n$  is the  $i$ th undamped mode,  $p_i(t) \in \mathbb{R}$  is the response of the  $i$ th mode, and  $n$  is the number of retained modes. The output is given by

$$Y_k = Y(t_k) = Hq(t_k) = Hq_k \quad (18)$$

where  $H$  determines the measured degrees of freedom. The residual is generated as that part of the response not in the modal subspace. The response is projected onto the modal subspace using

$$P = H\Phi[H\Phi]^\dagger \quad (19)$$

where  $[\bullet]^\dagger$  denotes the pseudo inverse and  $\Phi$  is the modal matrix whose columns are the modes. Generally only a small number of modes are used, and thus  $\Phi$  is a rectangular matrix. The residual consists of the response not in the subspace, and is generated as

$$\varepsilon_k = [I - P]Y_k = [I - P]Y_k^{(1)}. \quad (20)$$

This is the residual at a single time sample, and should be compared to Equation (15) for the parity space approach. To be consistent with the parity space approach all of these residuals in the time window of interest need to be computed. Furthermore, the modal approach does not use any information concerning the input force.

## 6 Residual Testing

The result from the parity space test, Equation (15), is a set of residuals,  $\varepsilon$ , where the  $k$  subscript has now been dropped. The mean of these residuals should be zero if there are no faults, and the model of the structure is sufficiently accurate. Modeling errors often appear as changes to the mean of the response and therefore such errors will degrade the performance of the

sensor fault detection. Fortunately the sensitivity of mode shapes to parameter errors is usually quite small. A full sensitivity analysis of the effect of modeling errors could be performed; however, the key conclusion is that the errors in the modal model must be smaller than the additive sensor faults. An alternative is possible, if measurements are available that include modeling error, but when all of the sensors are known to be functioning. In this case the mean values due to the modeling error may be subtracted before the residuals are tested. A similar approach to the residual testing may be used for the residuals generated using the modal model, Equation (20), but the following will concentrate on the parity space approach. Basseville [3,4] considered the statistical aspects in more detail. Hypothesis testing is standard in the statistics literature [13] and only a brief summary will be presented here. The covariance matrix is assumed known, although in practice this matrix will be estimated from the data.

The faults are combined into a single vector, so that

$$M_X(\Gamma)F_X + M_Y(\Xi)F_Y = M\Upsilon \quad (21)$$

where  $\Upsilon = \begin{Bmatrix} F_X \\ F_Y \end{Bmatrix}$  and  $M = [M_X(\Gamma) \ M_Y(\Xi)]$ . If the noise sequences,  $V_k$  and  $W_k$ , are Gaussian then the residuals,  $\varepsilon$ , will be also Gaussian (since the sum of independent Gaussian random variables is Gaussian, [13]) with mean  $N^T M \Upsilon$ . Assume that the covariance matrix is given by  $\Sigma$ . The likelihood ratio test is now used to determine which of the hypotheses  $\Upsilon = 0$  and  $\Upsilon \neq 0$  is most likely to be true. If  $f_\Upsilon(\varepsilon)$  is the probability density function of the residuals, then the log-likelihood function is given by

$$\begin{aligned} l_\Upsilon(\varepsilon) &= -2 \ln f_\Upsilon(\varepsilon) \\ &= \{\varepsilon - N^T M \Upsilon\}^T \Sigma^{-1} \{\varepsilon - N^T M \Upsilon\}. \end{aligned} \quad (22)$$

Usually the best estimate of  $\Upsilon$  is found by maximizing the probability density function, or equivalently by minimizing the log-likelihood function. From Equation (22) this is equivalent to the weighted least squares solution, and is

given by

$$\hat{\Upsilon} = F^{-1} M^T N \Sigma^{-1} \varepsilon \quad (23)$$

where

$$F = M^T N \Sigma^{-1} N^T M \quad (24)$$

is the Fisher information matrix. Note that

$$l_{\hat{\Upsilon}}(\varepsilon) = \min_{\Upsilon} l_{\Upsilon}, \quad f_{\hat{\Upsilon}}(\varepsilon) = \max_{\Upsilon} f_{\Upsilon}(\varepsilon). \quad (25)$$

To test whether the faults are indeed zero, that is to choose between  $\Upsilon = 0$  and  $\Upsilon \neq 0$ , the ratio of the probability density function when  $\Upsilon = \hat{\Upsilon}$  and when  $\Upsilon = 0$  is considered. A test statistic [13] has a known probability density function and so the probability that the test statistic assumes a measured value may be estimated. In this case the test statistic is

$$t \equiv 2 \ln \frac{f_{\hat{\Upsilon}}(\varepsilon)}{f_0(\varepsilon)} = \varepsilon^T \Sigma^{-1} N^T M F^{-1} M^T N \Sigma^{-1} \varepsilon. \quad (26)$$

This test statistic ( $t$ ) is distributed as a  $\chi^2$  random variable with  $\dim(\Upsilon)$  degrees of freedom.  $t$  is only  $\chi^2$  if  $\Sigma$  is constant. In practice,  $\Sigma$  is estimated from the measurements, and so strictly speaking  $t$  is not  $\chi^2$ . However, the errors introduced from this approximation are expected to be small.

The above test may be used to detect faults, that is to determine whether  $\Upsilon = 0$  or not. Suppose the possible sensors are now split into 2 sets, namely the ones assumed to be working,  $\Upsilon_w$ , and those assumed to be faulty,  $\Upsilon_f$ . Thus,

$$M\Upsilon = [M_w \ M_f] \begin{Bmatrix} \Upsilon_w \\ \Upsilon_f \end{Bmatrix}. \quad (27)$$

The objective is to test whether  $\Upsilon_w = 0$  or  $\Upsilon_w \neq 0$ , where  $\Upsilon_f$  is assumed to be an unknown vector. This is sometimes called the *sensitivity* test. If  $f_{\Upsilon_w, \Upsilon_f}(\varepsilon)$  is the probability density function of the residuals in terms of the working and

faulty sensor inputs, then the test statistic is now

$$t_w \equiv 2 \ln \frac{f_{\hat{\Upsilon}_w, 0}(\varepsilon)}{f_{0,0}(\varepsilon)} = \varepsilon^T \Sigma^{-1} N^T M_w F_{ww}^{-1} M_w^T N \Sigma^{-1} \varepsilon. \quad (28)$$

where

$$f_{\hat{\Upsilon}_w, 0}(\varepsilon) = \max_{\Upsilon_w} f_{\Upsilon_w, 0}(\varepsilon), \quad F_{ww} = M_w^T N \Sigma^{-1} N^T M_w. \quad (29)$$

The test statistic,  $t_w$ , is distributed as a  $\chi^2$  random variable with  $\dim(\Upsilon_w)$  degrees of freedom.

The above test statistic has been developed based on the equations for the residuals obtained from the parity space approach. However, exactly the same procedure may be applied to the modal residuals. In this case only additive faults on the output (or sensors) are considered (note that in practice this is also the case for the parity space approach). In the development  $N^T$  is replaced with  $(I - P)$ .

## 7 Simulated Example

The proposed approaches will be tested on a simulated example of a cantilever beam excited at its tip, shown in Figure 1. The beam is 1 m long, 2.5 cm thick, and 5 cm wide and the material properties of the beam are those of steel (a Young's modulus of 210 GN/m<sup>2</sup>, a mass density of 7850 kg/m<sup>3</sup>). The beam is simulated using 10 finite elements, and the output responses are the nodal displacements. The equations of motion are reduced by retaining only the lower 5 undamped modes in order to perform the numerical integration for the time response. Modal damping of 1% is included. A half sine pulse force of 4 ms duration is applied at the tip, which simulates an impact excitation, and also excites the higher modes.

For illustrative purposes only the one fault case has been simulated, although the multiple fault case is considered in the experimental example. Random noise is added to all of the responses, and this noise is taken from a uniform

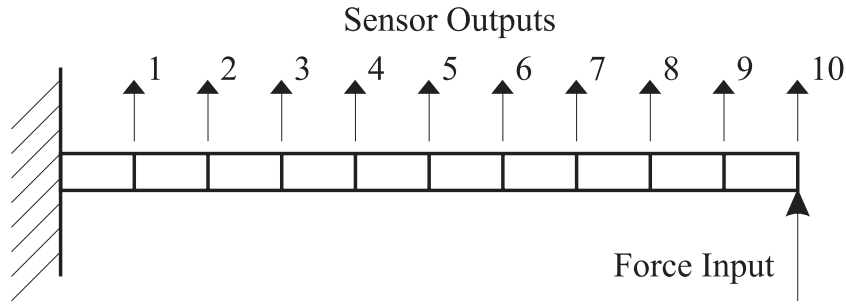


**Figure 1** A schematic of the cantilever beam example.

**Table 1** Results for the simulated example with an additive fault to sensor 6.

	<i>Parity Space Residuals</i>	<i>Modal Residuals</i>
	<i>Global Tests</i>	
<i>H0</i>	10.16	5.00
<i>H1</i>	$6.72 \times 10^3$	$3.49 \times 10^3$
<i>Sensor Number</i>	<i>Sensitivity Tests (<math>\times 10^3</math>)</i>	
1	0.0883	0.0582
2	0.0984	0.0480
3	0.3202	0.1543
4	0.0291	0.0325
5	2.4428	1.3981
<b>6</b>	<b>6.7140</b>	<b>3.4913</b>
7	2.9133	1.4764
8	0.0923	0.0215
9	0.3209	0.2016
10	0.4763	0.2704

distribution, which can be positive or negative, with a maximum magnitude of 2% of the maximum response from all the sensors. A fault is introduced into sensor 6, such that the response has an additive error of 5% of the maximum response of all the sensors. A total number of 10,000 data points were generated and used in the computation of the test covariance matrix. Both the modal residual and parity space approaches were tested. In all the simulations the full parity space dimension was used. Investigating the effect of using different parity space dimensions is outside the scope of the current paper. Table 1 shows the global tests as well as the sensitivity tests for the case of an additive fault on sensor 6 for both residuals. The quantities given are the likelihood values,

**Table 2** Frequencies and damping ratios identified using the BR algorithm.

<i>Frequency (Hz)</i>	<i>Damping (%)</i>
60.72	0.13
156.32	0.17
190.66	0.16
229.19	0.20
287.11	0.10

and so large values mean that the corresponding hypothesis is more likely.  $H_0$  is the hypothesis that  $\Upsilon = 0$  and  $H_1$  is the hypothesis that  $\Upsilon \neq 0$ . From the numerical values that the test clearly detects the fault and the sensitivity tests locate the faulty sensor as the maximum value of the test. Notice that all the sensitivity tests have been affected by the fault on a single sensor as indicated by the high values for the other sensors.

## 8 Experimental Example

The structure considered in this study consists of a suspended steel subframe used extensively in modal identification studies [1]. The structure is excited at two different locations using random noise inputs, and 28 accelerometers were used to measure the time response. The analysis was performed in the 0–500 Hz frequency range and 32,000 data points per channel were collected at a 1024 Hz sampling frequency. All 28 sensors were used to identify the experimental natural frequencies, damping ratios, and mode shapes from the first 3000 data samples. The Balanced Realization algorithm using data correlations was used for the identification [2]. Table 2 shows the first five

identified modes that were retained for the analysis (up to 300 Hz).

The parity space method has been applied to this structure with three different sensor faults: 10% and 20% additive faults on sensors 6 and 20 respectively, and then 10% and 20% additive faults on sensors 6 and 20 simultaneously. A total of 3000 data points were used in the computation of the test covariance matrix. In all cases the full parity space dimension was used. The minimum window size was used ( $p=1$ ) due to the large number of sensors available. Figures 2 and 3 show the results for all 28 sensors, and demonstrate that the method successfully isolates the faulty sensors in the single fault cases. The residual testing technique was also applied to the modal residuals and a similar behavior was observed, as shown in Figures 4 and 5.

As the number of sensors available is reduced then so too is the quality of the fault detection. Figures 6–8 show the effect of reducing the total

number of sensors to 15, 10, and 8 respectively, for a 10% change in sensor 6. Results are shown for the parity space residuals, but those for the modal residuals are very similar. Of course the choice of sensors may not be optimum, particularly if the resulting mode shapes cannot be separated readily, and this choice becomes more critical as the number of sensors is reduced. Note that for the 8 sensor case the number of modes used had to be reduced to 4.

Figure 9 shows the results for the multiple fault case for the parity space residuals (the results for the modal residuals are very similar). The sensor with the largest error is clearly identified, although it is difficult to isolate multiple faults. This is not a limitation of the method since it has been assumed at the start that only a single sensor was faulty. For multiple faults, one needs to use either the subset selection technique, as mentioned in Section 2, or an exhaustive search to find the faulty sensors. Because of the small number of sensors in this example, all

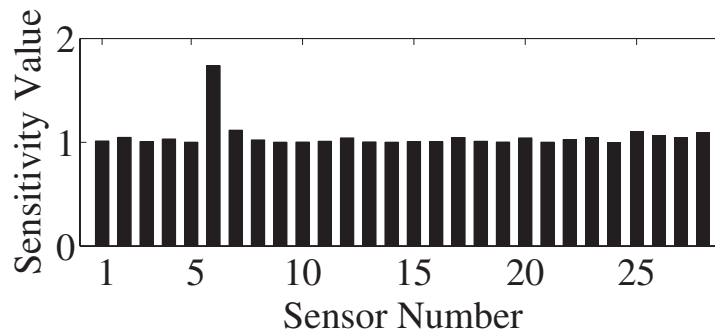


**Figure 2** Experimental subframe example using parity space residuals: 10% change in sensor 6.

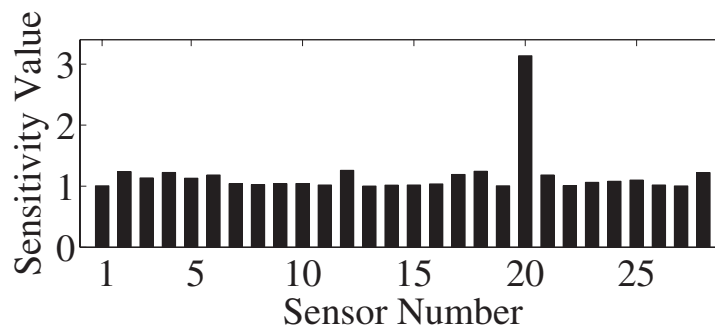


**Figure 3** Experimental subframe example using parity space residuals: 20% change in sensor 20.

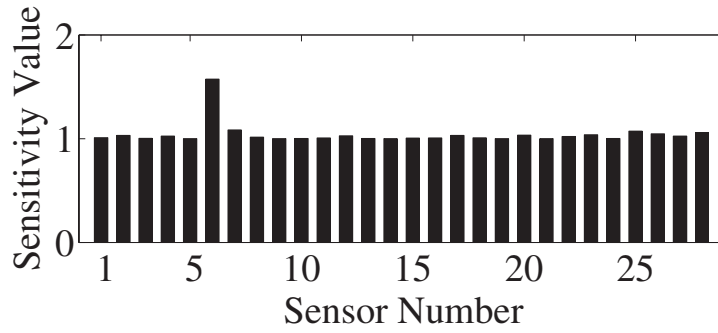


**Figure 4** Experimental subframe example using modal residuals: 10% change in sensor 6.

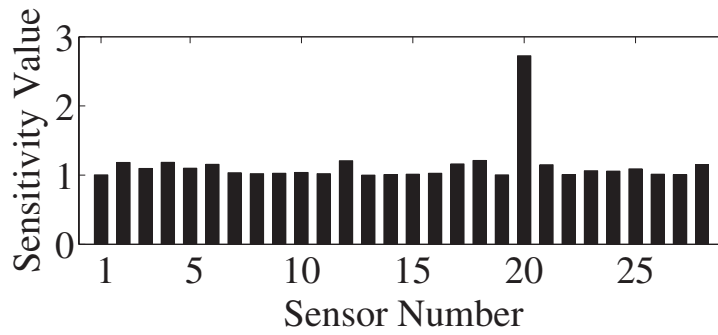


**Figure 5** Experimental subframe example using modal residuals: 20% change in sensor 20.

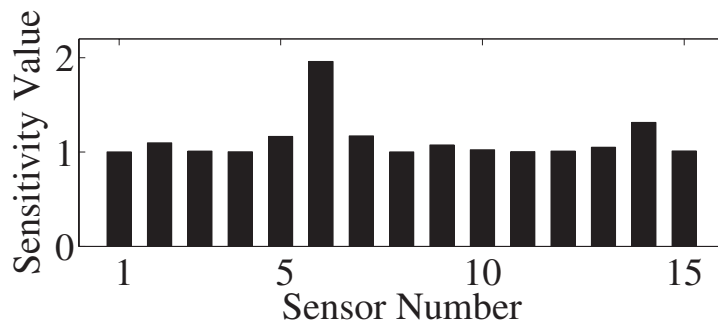


**Figure 6** Experimental subframe example using parity space residuals using 15 sensors: 10% change in sensor 6.

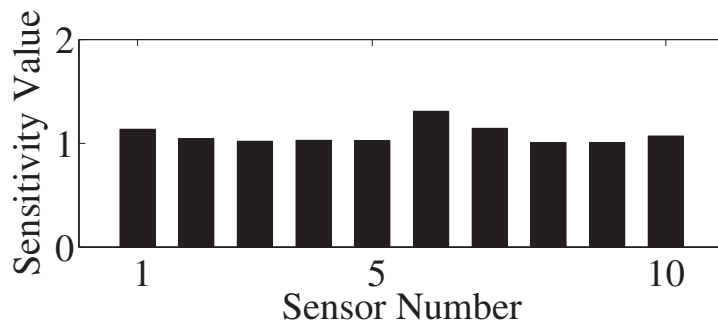


**Figure 7** Experimental subframe example using parity space residuals using 10 sensors: 10% change in sensor 6.

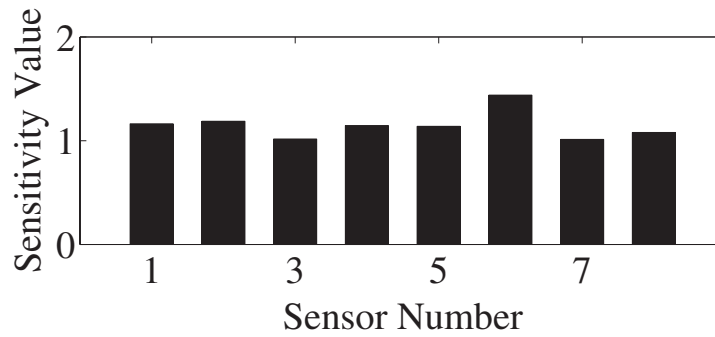


**Figure 8** Experimental subframe example using parity space residuals using 8 sensors and 4 modes: 10% change in sensor 6.

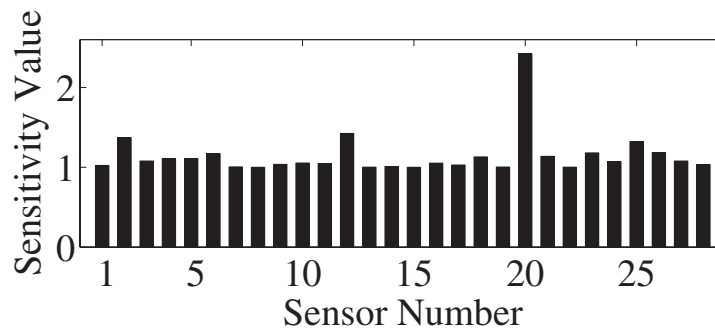


**Figure 9** Experimental subframe example using parity space residuals: 10% change in Sensor 6 and 20% change in sensor 20.

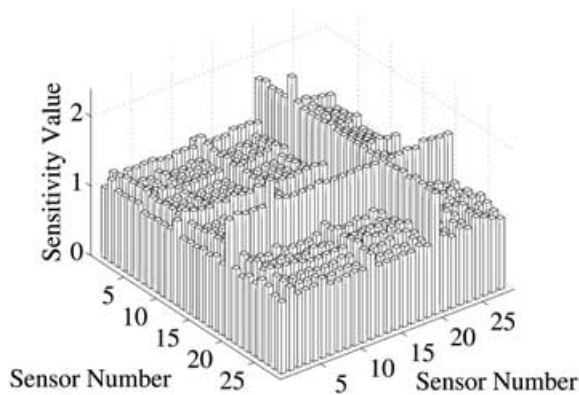


**Figure 10** Experimental subframe example using parity space residuals and assuming two sensors are faulty: 10% change in sensor 6 and 20% change in sensor 20.

subsets of two sensors may be tested exhaustively. Figure 10 shows the sensitivity test for all pairs of sensors. The highest value of the test is clearly at the correct pair of sensors, namely sensors 6 and 20.

## 9 Conclusions

Two residual generation schemes have been proposed for the sensor validation problem under additive faults, namely the parity space approach and the modal filtering technique. The performance of the residuals, in the examples given in this paper, is very similar. However, the parity space approach only requires an input–output model, damping may be included easily, and excitation force may be included explicitly, if it is available. The residual evaluation is based on statistical arguments and the problem of fault detection is transformed into the problem of detecting the change in the mean of a Gaussian variable with known covariance matrix. This problem was solved using likelihood ratio tests. The procedure was first illustrated on a simulated cantilever beam excited at its tip, and then on an experimental test consisting of a subframe structure. Both residuals perform well. The problem of

multiplicative faults will be addressed in a future paper.

## Acknowledgment

Prof. Friswell acknowledges the support of a Royal Society-Wolfson Research Merit Award.

## References

1. Abdelghani, M., Chou, C.T. and Verhaegen, M. (1997). Using subspace methods in the identification and modal analysis of structures. *15th International Modal Analysis Conference*, Orlando, Florida, USA, 1392–1398.
2. Abdelghani, M., Goursat, M., Biolchini, T., Hermans, L. and van der Auweraer, H. (1999). Performance of output-only identification algorithms for modal analysis of aircraft structures. *17th International Modal Analysis Conference*, Kissimmee, Florida, USA, 224–230.
3. Basseville, M. (1997). Information criteria for residual generation and fault detection and isolation. *Automatica*, 33(5), 783–803.
4. Basseville, M. (1998). On-board component fault detection and isolation using the statistical local approach. *Automatica*, 34(11), 1391–1415.
5. Dunia, R., Qin, S.J., Edgar, T.F. and McAvoy, T.J. (1996). Identification of faulty sensors using principal component analysis. *AIChE Journal*, 42(10), 2797–2812.
6. Dunia, R. and Qin, S.J. (1998). Subspace approach to multidimensional fault identification and reconstruction. *AIChE Journal*, 44(8), 1813–1831.
7. Friswell, M.I. and Inman, D.J. (1999). Sensor validation for smart structures. *Journal of Intelligent Material Systems and Structures*, 10(12), 973–982.
8. Friswell, M.I., Penny, J.E.T. and Garvey, S.D. (1997). Parameter subset selection in damage location. *Inverse Problems in Engineering*, 5(3), 189–215.
9. Friswell, M.I., Mottershead, J.E. and Ahmadian, H. (1998). Combining subset selection and parameter constraints in model updating. *Journal of Vibration and Acoustics*, 120(4), 854–859.
10. Lallement, G. and Inman, D.J. (1995). A tutorial on complex eigenvalues. *13th International Modal Analysis Conference*, Nashville, TN, 490–495.
11. Meirovitch, L. (1990). *Dynamics and Control of Structures*, John Wiley & Sons.
12. Millar, A.J. (1990). *Subset Selection in Regression*, Monographs on statistics and applied probability 40, Chapman and Hall.
13. Montgomery, D.C., Runger, G.C. and Hubele, N.F. (2001). *Engineering Statistics*, John Wiley & Sons, New York, 2nd Edn.
14. Qin, S.J., Yue, H. and Dunia, R. (1997). Self-validating inferential sensors with application to air emission monitoring. *Industrial & Engineering Chemistry Research*, 36, 1675–1685.